HYDROGEN MASERS. II: MWC349.

Vladimir S. Strelnitski ^{1,2}, Howard A. Smith ², and Victor O. Ponomarev ³

Submitted to the Astrophysical Journal, Part 1

¹ New Mexico Institute of Mining and Technology, Socorro, NM 87801

 $^{^2}$ Laboratory for Astrophysics, National Air and Space Museum, Smithsonian Institution, Washington, DC 20560

³ P.N. Lebedev Physical Institute, 117924 Moscow, Leninsky prospect 53, Russia

ABSTRACT

The conditions of masing and lasing in the hydrogen recombination lines (HLR) in the disk and outflow of MWC349 are studied. Comparison of the complete set of the observed α -lines, from H2 α through H92 α , with simple models of optically thin spontaneous emission shows that observable HRL masing in this source is limited to the interval of the principal quantum numbers $n \approx 10-36$.

We use our analytical and numerical results for the conditions of optimum masing (Strelnitski $et\,al.$ 1995b; "Paper 2"), and the morphological parameters of a photoevaporized circumstellar disk modelled by Hollenbach $et\,al.$ (1994), to obtain analytical approximations and quantitative estimates for the expected unsaturated maser gain and the degree of saturation in HRL masers in the disk of MWC349. It is shown that the unsaturated maser gains of the IR and optical HRL lasers should be very high but in fact all of these transitions are strongly saturated. Due to saturation, their relative intensity with respect to the spontaneous emission should steeply drop toward smaller n's which explains why optical and near infrared HRL lasers are not seen in MWC349. This result is quite general and makes the prognosis for observable high-frequency lasers in other sources pessimistic as well. An exception might arise due to special geometry, if lasing were confined to very small solid angles.

We show that weak masing from the *outflow* of MWC349 is only possible in low n α -lines ($n \lesssim 20$ –30), and then only if the outflow begins much closer to the central star than the Hollenbach *et al.* model predicts ($\approx 3 \cdot 10^{15}$ cm). We therefore conclude that maser emission from the *disk*, rather than from the outflow, is responsible for the observed weak amplification of the "pedestal" spectral components in the α -lines with $n \lesssim 40$. The fluxes in the lower frequency α -lines are well explained by spontaneous emission from the outflow, with proper corrections for free-free absorption.

We review the current state (and prospects) of observations of masing and lasing hydrogen β -lines in MWC349. We argue in favor of "close in n," rather than "close in frequency" α/β pairs for intensity analysis, when maser amplification is present.

 $Subject\ headings:\ stars: early-type--stars:\ individual\ (MWC349)--stars: mass\ loss\ --masers--radio\ recombination\ lines$

1. INTRODUCTION

MWC349, a well-known variable emission line star (V 1478 Cyg) with high IR excess and the brightest stellar radio continuum source in our Galaxy, recently became the first known hydrogen maser in space. Martin-Pintado $et\,al.$ (1989a,b) detected strong, double-peaked emission in its mm hydrogen recombination lines (HRL), and even stronger submm double-peaked lines were subsequently detected by Thum $et\,al.$ (1994a,b). Martin-Pintado $et\,al.$ (1989a) presented arguments for the maser nature of the detected lines and demonstrated the principal possibility of high-gain masing in these lines in the dense ionized outflow from the star, but failed to explain the observed spectral pattern kinematically. Ponomarev $et\,al.$ (1989) attempted to explain this pattern, ascribing one of the spectral peaks to the outflow and another one to the partly ionized, infalling circumstellar disk. However, later, with new observational evidence, several authors (Gordon 1992; Planesas $et\,al.$ 1992; Thum $et\,al.$ 1992) were able to successfully ascribe both peaks to a circumstellar $Keplerian\,disk.$

The masing Keplerian disk model has further been elaborated upon by Thum $et\,al.$ (1994a,b) and by Ponomarev $et\,al.$ (1994). The slight observed variations of the $35\alpha-30\alpha$ line widths with intensity, and the deep dip between the two spectral peaks of 30α , were respectively attributed by Thum $et\,al.$ (1992) and by Ponomarev $et\,al.$ (1994), to the effects of unsaturated maser amplification. Earlier, however, Ponomarev $et\,al.$ (1991) estimated that the 30α line should be at the threshold of saturation. Thum $et\,al.$ (1992; 1994a,b) found several observational manifestations of increasing saturation toward higher frequency submm lines and connected them with a decreasing role of collisional relaxation with increasing line frequency. Saturation seems to be a key issue for predicting HRL lasing in the IR and optical; therefore it is one of the central topics of this paper and of the previous one (Strelnitski $et\,al.$ 1995b; "Paper 2").

Originally the mm and submm HRLs in MWC349 were decomposed into a "masing" (double-peaked) component associated with the disk, and a "thermal" (pedestal) component attributed to the outflow (Thum et al. 1992). However, several recent papers claimed weak masing in the pedestal component too (Martı́n-Pintado et al. 1994a,b; Thum et al. 1994b; 1995). In the present paper we attempt to develop a self-consistent model of HRL masing and lasing in the disk and outflow of MWC349, in order to explain the full set of existing observations and to predict the properties of yet unobserved, potentially lasing HRLs at higher frequencies.

We summarize, in Section 2, the observed fluxes in most of the hydrogen α -lines which have so far been detected in this source — from H α , at 6563 Å, through 92 α , at 3.6 cm. Comparison of the observed fluxes with simple theoretical models for optically thin spontaneous emission provides further evidence for masing, and delineates the limits of "active" frequencies.

Section 3 is devoted to the interpretation of the double-peaked maser lines. Using the approach to saturation analysis developed in Paper 2, we obtain a reliable observational estimate of the degree of saturation for the 30α maser, confirming the rough previous suggestions that this line should be at the threshold of saturation. We use the morphological parameters of the photoevaporation disk model of Hollenbach et al. (1994), and our analytical and numerical results concerning maser gains in HRLs, to calculate the expected values of the unsaturated gain and the degree of saturation for α -lines in the interval $5 \lesssim n \lesssim 35$. We show that all the IR α -line lasers in MWC349 should be strongly saturated, in accordance with the saturation tendencies revealed by Thum et al. (1994a,b) from their observations of mm and submm masers. The expected maser-to-spontaneous intensity ratios for these saturated lines steeply decrease toward lower n, providing further support for our previous conclusion (Strelnitski et al. 1995a) that detectable double-peaked α -line lasing in MWC349 should extend from the submm into the IR domain — and then vanish somewhere around $n \approx 10$. We use the qualitative ideas about the interaction of saturated masing lines developed in Paper 2 to explain the observed "clustering" of the mm and submm lines near a single value of the separation of two spectral peaks in radial velocity.

An analysis of the conditions for masing in the MWC349 outflow (Section 4) brings us to the conclusion that although weak masing in α -lines is possible here for $n \lesssim 30$, the observed increase of the pedestal relative intensity toward lower n is more probably due to amplification in the disk. The bulk of the higher n pedestal lines is fairly well explained by optically thin, spontaneous emission from the outflow, when proper corrections for the free-free absorption in the lines are included.

In Section 5 we review the observational and theoretical situation of the masing hydrogen β -lines. We demonstrate that, in accordance with our model predictions, the only known weakly masing double-peaked β -line (32 β) forms in the disk near the corresponding α -lines of close n. We argue that, when

masing is present, observations of the "close in n" α/β pairs should be more instructive than observations of "close in frequency" pairs. A prognosis for detecting other β -line masers in MWC349 is given.

In Appendix 1, we argue that previous attempts to prove the presence of masing in mm HRLs in MWC349 are not fully satisfactory, and we give a more rigorous proof using two observed parameters of 30α — the flux, and the interferometric angular scale of the emitting medium — and using only very general model considerations about maser geometries in a Keplerian disk.

In Appendix 2, we derive a simple expression for the β/α line spontaneous emissivity ratio. It can be useful for estimating whether or not effects of optical depth (positive or negative) are present in the observed β/α intensity ratio.

2. SUMMARY OF THE HYDROGEN α -LINE FLUXES IN MWC349

In Figure 1 we plot the integrated intensities of the most of hydrogen recombination α -lines observed so far in MWC349 (we omitted some lines for the sake of the figure's clarity).

The fluxes in clearly observed double-peaked, narrow-band components are shown with dots; those in single-peaked, broad-band components ("pedestals") — with squares. The latter symbol is also used for poorly resolved profiles and for profiles with only barely resolved double-peaked components. Filled symbols mark single observations (when several are known, we normally choose the brightest one); open symbols, averages for some period of observations (taken from Thum et al. 1992; 1994a). Three optical and near IR lines ($\text{H}\alpha$, $\text{P}\alpha$ and $\text{B}\alpha$) were corrected for interstellar and circumstellar extinction using the extinction curve given by Thompson et al. (1977).

The two solid lines in Fig. 1 show the calculated spontaneous emissivity ratios for the Baker and Menzel's "Case B", for two extreme density values possible in the emission line region of MWC349. The difference between the two lines is not significant. Since these theoretical lines show only ratios of emissivities, their position along the ordinate is arbitrary. The broken line gives the spontaneous emissivity ratios, corrected for free-free absorption, which is important for low-frequency ($n \gtrsim 30$) lines. The correction procedure is described in Section 4. The position of this theoretical line along the ordinate is also arbitrary.

Although the observational data in Fig. 1 are not homogeneous and belong to (or are averaged over) different epochs, we can clearly see some important tendencies.

The most striking fact is that theoretical curve for optically thin spontaneous emission, with only the correction for free-free absorption, describes satisfactorily the observed fluxes in almost all the *pedestal* components, from the highest frequency optical and near IR lines to the lowest frequency radio lines — more than 4 decades in frequency and almost 12 decades in flux!

In contrast, the mm and submm double-peaked lines (dots in Fig. 1) lie, as a group, considerably higher than the spontaneous emission curve. This may be regarded as strong, though indirect, evidence of their being amplified. The pedestal components of the two submm lines, 26α and 21α , recently detected by Thum et al. (1994b), also show evidence of amplification in Fig. 1.

To date, 10 double-peaked mm and submm hydrogen recombination lines have been reported in MWC349 (Martin–Pintado $et\,al.$ 1989a,b; Thum $et\,al.$ 1994a,b; 1995): nine α -lines — 36α , 35α , 34α , 31α , 30α , 29α , 27α , 26α , 21α , and one β -line — 32β . The 36α line is the lowest frequency α -line where the double-peaked component first appears with intensity comparable to the pedestal component. Both the peak flux density S of the double-peaked component and its integrated flux F increase with line frequency, attaining $S_{max}\approx 300\,\mathrm{Jy}$ and $F\approx 1\cdot 10^{-20}\,\mathrm{W\,cm^{-2}}$ by 21α (Thum $et\,al.$ 1994b).

The tantalizing question naturally arises: how far into the still unexplored IR domain does the phenomenon of double-peaked masing extend? There is one evident limit: the well known optical and near IR lines seem to be satisfactorily described by optically thin, or slightly thick, spontaneous emission (Fig. 1 and also Thompson et al. 1977; Hamann and Simon 1986). Smith et al. (1995) and Strelnitski et al. (1995a) recently undertook to narrow the gap of unobserved lines between submm and near IR. Smith et al. detected 6α (12.37 μ m) and 7α (19.06 μ m) on the IRTF telescope, and Strelnitski et al. marginally detected 10α (52.53 μ m) and obtained an upper limit for 15α (169.4 μ m) with the KAO observatory. Fig. 1 shows that whereas the 7α line lies very close to the optically thin spontaneous curve, as other optical and near IR lines do, the 10α is ≈ 4 times brighter than the spontaneous curve predicts. The 15α flux upper limit lies about 10 times higher than the spontaneous curve at this frequency.

Though Strelnitski et al. (1995a) could not spectrally resolve 10α to see whether or not it is double-peaked, they conjecture, on the basis of the line's flux excess, that observable lasing from MWC349 might extend into the far IR down to $n \approx 10$. However, at lower n detectable lasing definitely seems to vanish.

An important characteristic of the masing mm and submm double-peaked lines is their relative intensity with respect to the pedestal. Along with the increase of the peaks' absolute intensity, the ratio I_c/I_{pk} of the pedestal's intensity at the central dip between the peaks to the peaks' intensity decreases from the threshold 36α line, where $I_c/I_{pk} \approx 1$, down to 30α , where this ratio falls to ≈ 0.07 (Ponomarev et al. 1994). It is seen from the recent observations by Thum et al. (1994b) that I_c/I_{pk} is still low at 26α (≈ 0.06), but at 21α it becomes much higher, > 0.2.

The following questions thus have to be answered:

- (1) Why does the double-peaked maser first appear at 36α ?
- (2) Why does its relative intensity with respect to the pedestal component first increase and then decrease with decreasing n?
- (3) Why do the observable masers, both the double-peaked and the pedestal ones, eventually vanish with decreasing n?

We address the double-peaked and the pedestal components separately in the two following sections.

3. THE DOUBLE-PEAKED COMPONENT: DISK MASERS

3.1. Morphological Model

We analyse the conditions for HRL masing in MWC349 in the framework of the Hollenbach $et\,al.$ (1994) morphological model of a circumstellar disk photoevaporized by a massive hot central star. According to that model, in the case where the "fast" stellar wind from the hot central star has normal parameters, photoevaporation of the disk by L_c photons from the star creates two distinct regions:

(1) the inner region, $R \leq R_g = 10^{14} M_*/M_{\odot}$ (cm), — a nearly static ionized atmosphere of the disk whose scale hight H increases with the radial distance R as

$$H(R) = R_g \left(\frac{R}{R_g}\right)^{3/2} \tag{3.1.1}$$

and the base number density of electrons decreases with R as

$$N_{e0}(R) = 5.7 \cdot 10^{29} \Phi_{49}^{1/2} R^{-3/2} \text{ cm}^{-3}$$
(3.1.2)

in the bulk of the atmosphere, except in its innermost part where the density increases toward the center somewhat faster ($\propto R^{-9/4}$); Φ_{49} here is the star's Lyman continuum photon luminosity, in 10^{49} photon/s;

(2) the outer region, $R \geq R_g$ — the "disk wind," freely outflowing ionized gas. We assume for MWC349-A: $M_* = 26 M_{\odot}$ (Ponomarev *et al.* 1994), thus $R_g \approx 3 \cdot 10^{15}$ cm. The quantity Φ_{49} is more difficult to determinate for stars as peculiar as MWC349-A; therefore we normalize Eq. (3.1.2) on the 30α line. We do so by adopting $2R\left(30\alpha\right) = 1.2 \cdot 10^{15}$ cm (the interferometric distance between the two hot spots, corresponding to the two spectral peaks, Planesas *et al.* 1992), and $N_{e0}\left(30\alpha\right) = 4 \cdot 10^7 \, \mathrm{cm}^{-3}$ (the optimum electron density for the amplification of this line at $T_e = 10^4 \, \mathrm{K}$; Paper 2). This fixes Φ_{49} in Eq. (3.1.2) at the realistic value of $\Phi_{49} \approx 1.1$. Thus, we adopt for the quasi-static part of the disk [dropping the sub-index "0," spreading thereby the $N_{e0}(R)$ value over the thickness H(R)]:

$$N_e(R) = 5.9 \cdot 10^{29} \, R^{-3/2} \, \text{cm}^{-3} \,.$$
 (3.1.3)

Combining this with the approximation for the optimum amplification density derived in Paper 2 (good over the whole interval $5{,}000\,\mathrm{K} \,{}^<_{\sim}\, T_e \,{}^<_{\sim}\, 10{,}000\,\mathrm{K}$):

$$N_e^{max} \approx 8 \cdot 10^{15} \, n^{-5.7} \,, \tag{3.1.4}$$

we obtain the following approximation for the radial distance of the maximum unsaturated amplification:

$$R_{max} \approx 1.8 \cdot 10^9 \, n^{3.8} \, \text{cm} \,.$$
 (3.1.5)

The values of R_{max} for the two extreme lines considered here, 35α and 5α , differ by about 3 orders of magnitude (Fig. 2). They are, however, both located within the static atmosphere.

3.2. Unsaturated Maser Gain

In the interval of R_{max} considered here the maximum amplification coherent path length (with respect to the radial velocity — the chord l_{max} in the Keplerian disk; cf. Paper 1) — is equal to R_{max} to within a factor of order unity. Thus the maximum unsaturated optical depth can be estimated as

$$\tau_0^{max} \approx k_{net}^{max} l_{max} \approx k_{net}^{max} R_{max} . \tag{3.2.1}$$

Substituting into Eq. (3.2.1) R_{max} from Eq. (3.1.5) and k_{net}^{max} from Eqs. (3.1.4) and (3.1.5) of Paper 2, we find

$$\tau_0^{max} \approx -2 \cdot 10^2 \frac{n^{-4.2}}{10} \qquad (T_e = 10^4 \,\mathrm{K}) ,$$

$$\tau_0^{max} \approx -1 \cdot 10^3 \frac{n^{-4.7}}{10} \qquad (T_e = 5 \cdot 10^3 \,\mathrm{K}) .$$
(3.2.2)

$$\tau_0^{max} \approx -1 \cdot 10^3 \frac{n^{-4.7}}{10} \qquad (T_e = 5 \cdot 10^3 \,\mathrm{K}) \,.$$
 (3.2.3)

These equations show, first of all, that there should be a threshold principal quantum number (frequency) for α -line masing in the disk — the highest value of $n \equiv n_{thresh}$ for which τ_0^{max} first becomes $\stackrel{>}{\sim} 1$. Eq. (3.2.2) gives, for example, $\tau_0^{max}(36\alpha) \approx 0.9$, and this is in good agreement with the observed threshold of the double-peaked masing at $n \approx 36$. The cut-off of the masing at $n \approx 36$ is, in this model, an "optical" effect based on the interplay of the density dependence of maser gain with the density structure of the disk; it does not require a physical cut-off of the disk as it does in Thum's et al., 1994a, suggestion. We note, however, that in fact 36α is masing in our model at $R \approx 1 \cdot 10^{15}$ cm — not so far from the edge of the static atmosphere $(R_q \approx 3 \cdot 10^{15} \, \text{cm})$.

Eqs. (3.2.2) and (3.2.3) show also that τ_0^{max} steeply increases with decreasing n: from $\tau_0^{max} \sim 1$ at $n \approx 35$, through $\tau_0^{max} \sim 10^1$ at $n \approx 20$, through $\tau_0^{max} \sim 10^2$ at $n \approx 10$, and up to $\tau_0^{max} \sim 10^3$ at $n \approx 5$. Thus, if this photoevaporation disk model for MWC349 and the hydrogen population calculations are basically correct, the unsaturated maser gains in the IR and optical hydrogen recombination lines in MWC349 should be very high.

Why then are the observed fluxes in optical and near IR lines not extraordinarily high and are, in fact, close to the optically thin spontaneous theoretical curve, Fig. 1? To answer this question, we examine more closely the conditions of saturation for the disk masers.

3.3. Saturation: Observational Evidence

Ponomarev et al. (1991) briefly analysed the conditions of saturation in the $H30\alpha$ line in MWC349 and showed that, with the observed flux and the geometrical scale of the emitting region estimated by Martin-Pintado et al. (1989b) from temporal variations, this line is probably marginally saturated.

A more detailed analysis of the connection between the observed line parameters and the degree of maser saturation was given in Paper 2. It was shown that the solid angle of maser emission — the most undetermined free parameter in the previous saturation analyses by Thum et al. (1992; 1994a) can actually be excluded from final equations. Then the geometry of the problem can be reduced to some linear scale l, whose reliable estimate, for such a source as MWC349, can be taken directly from interferometric observations. The degree of saturation, as measured by the ratio of the actual average intensity in the source J to the "saturation intensity" J_s , was shown to be

$$\frac{J}{J_s} \approx 0.2 \left(\frac{D}{\text{kpc}}\right)^2 \left(\frac{n}{10}\right)^{4.7} \left(\frac{S}{\text{Jy}}\right) \left(\frac{10^{13} \text{ cm}}{l}\right)^2, \tag{3.3.1}$$

where D is the distance to the source, S is the observed flux density, and l is the amplification path length.

We apply now this condition of saturation to the double-peaked component of 30α in MWC349, for which Planesas et al. (1992) measured the angular separation of the "blue" and "red" hot spots: $\theta_s = 0.065$ arcsec. It is convenient, in this case, to pass from l in Eq. (3.3.1) to $\theta_l = (l/D)$ — the angular measure of l as it would be seen from Earth, had it been perpendicular to the line of sight:

$$\frac{J}{J_s} \approx 1 \cdot 10^{-7} \left(\frac{n}{10}\right)^{4.7} \left(\frac{S}{\text{Jy}}\right) \left(\frac{\text{arcsec}}{\theta_l}\right)^2. \tag{3.3.2}$$

To a factor close to unity the amplification chord length in a Keplerian disk with our parameters is $l \approx s/2$, thus, $\theta_l \approx 0.5\theta_s \approx 0.03$ arcsec. Substituting into Eq. (3.3.2) this value and also n = 30, $S_{30\alpha} \approx 25 \,\mathrm{Jy}$ (Thum *et al.* 1994a), we find: $J/J_s \approx 0.5$. This confirms the suggestion made before by Ponomarev *et al.* (1991) and by Thum *et al.* (1992; 1994a) that this line should be at the threshold of saturation.

We emphasize that the forgoing analysis of 30α saturation is based on the directly measured quantities — the flux density and the angular scale — and is only weakly model dependent. Unfortunately, direct measurement of the angular scale has only been done for the 30α double-peaked component so far, and we can not apply the above analysis to other lines to see how the degree of saturation changes with n. However, Thum et al. (1992; 1994a,b) draw attention to some observational indications of growing saturation toward higher frequency lines: some broadening of the lines and levelling off of the maser photon luminosity. In the framework of their saturation analysis (which was reduced to the evaluation of the "saturation temperature" T_s — an analogue of J_s) they find that maser saturation "becomes easier" toward lower n because T_s for them is smaller. These authors correctly notice, however, that such an analysis is insufficient: only comparison of a saturation parameter $(T_s \text{ or } J_s)$ with the corresponding expected parameters of radiation field in the source enables any statement about the degree of saturation in a masing line.

In the theoretical analysis of saturation given in the next two sections we shall show that the degree of saturation indeed grows toward higher frequency HRL transitions in MWC349, and it leads to important consequences concerning observability of HRL lasers.

3.4. Saturation: Theoretical Prognosis

Assuming the solid angle of maser radiation Ω to be constant along the amplification path, and ignoring spontaneous emission with respect to the maser emission in a strong maser, the *unsaturated* growth of the average intensity with $|\tau_0|$ is given by

$$J_u \approx \frac{\Omega}{4\pi} I_0 e^{|\tau_0|} \,, \tag{3.4.1}$$

where I_0 is the input intensity — the intensity of the continuum or spontaneous emission, whatever is brighter, at the frequency of the line. In the Raleigh-Jeans domain (all the lines in question fall into this domain) the input intensity due to continuum is $2kT_b^c/\lambda^2 \leq 2kT_e/\lambda^2$, where T_b^c is the continuum brightness temperature and λ_0 is the transition wavelength. It can also be shown (e.g.: Strelnitski 1974) that the input intensity due to spontaneous emission is $2k|T_x|/\lambda^2$ where T_x is the transition excitation temperature. Since $|\beta_{12}| \sim 1$ at the density of maximum maser gain (Paper 2), we have $|T_x| \approx T_e/|\beta_{12}| \sim T_e$. Considering that the exact value of I_0 is not very important when $|\tau|$ is high, we can thus assume

$$I_0 \approx \frac{kT_e}{\lambda_0^2},\tag{3.4.2}$$

It was shown in Paper 2 that the saturation intensity for an HRL maser can be represented as

$$J_s \approx \frac{2h\nu_0^3}{c^2} \frac{A_t + C_t + C_{21}}{A_{21}},$$
 (3.4.3)

where $A_t \equiv (A_{t1}^{-1} + A_{t2}^{-1})^{-1}$ and $C_t \equiv (C_{t1}^{-1} + C_{t2}^{-1})^{-1}$ are the harmonic mean values of the total Einstein A coefficient and of the total collision rate for the two maser levels, A_{21} is the Einstein A coefficient for the signal transition, and C_{21} is the rate of collisional relaxation between the maser levels. It was also

argued that, at the optimum density for maser amplification in a HRL, A_t in Eq. (3.4.3) can always be ignored as compared with $(C_t + C_{21})$ which, in its turn, can be approximated as

$$\delta \equiv (C_t + C_{21}) \approx 3 \cdot 10^{-9} \, n^5 \, N_e \,. \tag{3.4.4}$$

Substituting for N_e the approximation (3.1.4) for N_e^{max} ; using: $A_{n+1,n} \approx 6.3 \cdot 10^9 \, n^{-5} \, (\mathrm{s}^{-1})$ and $\nu_0 = c/\lambda_0 \approx 6.6 \cdot 10^{15} \, n^{-3} \, (\mathrm{s}^{-1})$ (the common approximations valid for $n\alpha$ -lines with $n \gg 1$); and neglecting A_t in Eq. (3.4.3), as compared with $(C_t + C_{21})$, we obtain from Eqs. (3.4.1) – (3.4.4), at a line's optimum density:

$$J_s \approx \frac{2h\nu_0^3}{c^2} \frac{\delta}{A_{21}} \approx 2 \cdot 10^{-2} \, n^{-4.7} \,,$$
 (3.4.5)

and

$$\frac{J_u}{J_s} \approx 0.3 \, n^{-1.3} \, \Omega \, \mathrm{e}^{|\tau_0|} \, .$$
 (3.4.6)

Note that Eq. (3.4.5) is valid over the whole temperature range considered here $(5,000 \,\mathrm{K} \lesssim T_e \lesssim 10,000 \,\mathrm{K})$, whereas the factor $\mathrm{e}^{|\tau_0|}$ makes Eq. (3.4.6) rather strongly temperature dependent.

The solid angle of maser radiation can be estimated in our disk model of MWC349 as

$$\Omega \approx \frac{0.5 R_{max} H}{l_{max}^2} \approx 0.5 \frac{H}{R_{max}} \approx 0.9 \cdot 10^{-8} R_{max}^{1/2} \approx 4 \cdot 10^{-4} n^{1.9}$$
. (3.4.7)

It is assumed in Eq. (3.4.7) that the "vertical" size of the masing hot spot is $\approx H$, and its "horizontal" size is $\approx 0.5 R_{max}$. The latter seems to be a reasonable estimate considering the radial density scale in the model disk (limiting the ring of maximum amplification), and the gradient of velocities in a Keplerian disk, as is directly shown by the numerical modeling of maser amplification in such a disk (Paper 1). The last two equalities in Eq. (3.4.7) are obtained by substituting H from Eq. (3.1.1), with $R_g \approx 3 \cdot 10^{15}$ cm, by assuming $R = R_{max}$, and by substituting Eq. (3.1.4) for R_{max} .

Combining Eqs. (3.4.6) and (3.4.7), we get, for the case of MWC349:

$$\frac{J_u}{J_s} \approx 1 \cdot 10^{-4} \, n^{0.6} \, \mathrm{e}^{|\tau_0|} \,.$$
 (3.4.8)

The exponential factor is decisive in Eq. (3.4.8). If the degree of saturation J_u/J_s is indeed ~ 1 at $n \approx 30$, where also $|\tau_0| \approx 6$ (both these results seem to be reasonable based on comparisons of *observations* with our models), then J_u/J_s should quickly become $\gg 1$ at smaller n's, because of the rapid increase of $|\tau|$ with decreasing n [cf. Eqs. (3.2.2-3)].

We therefore conclude that all the hydrogen IR and optical α -line lasers in MWC349 should be deeply saturated.

3.5. Observability of IR and Optical Lasers

It is shown (e.g.: Strelnitski 1974) that the output intensity of a saturated maser can be represented as

$$I_s \approx \frac{4\pi}{\Omega} J_s |\tau_0| \,, \tag{3.5.1}$$

where τ_0 is the *unsaturated* optical depth. In the case of a homogeneous amplification path of length l, τ_0 for a HRL is given by

$$\tau_0 = (k_c' + k_l^0) l , \qquad (3.5.2)$$

with k'_c being the continuum absorption coefficient at the line frequency and k^0_l being the unsaturated line absorption coefficient. However, for those HRL's that have been observed as strong masers $(n \lesssim 35)$ $k'_c \ll k^0_l$ (see Fig. 10 in Paper 2), hence we can ignore k'_c in Eq. (3.5.2) as compared with k^0_l and write:

$$\tau_0 \approx k_l^0 l = \frac{h\nu_0 B_{12}}{4\pi\Lambda\nu} N_1' b_1 \beta_{12} l , \qquad (3.5.3)$$

where B_{12} is the Einstein coefficient, $\Delta \nu$ is the line width, N'_1 is the LTE population of level 1, and b_1 , β_{12} are the usual departure coefficients.

Since the masing "hot spots" in MWC349 are not spatially resolved as yet, it is more convinient to discuss their observed radiation in terms of the flux density rather than intensity, even in terms of the flux density integrated over frequency — for easier comparison with spontaneous emission. The integrated flux density due to the portion of the source having a surface area $d\sigma$ and an outgoing intensity I at the line center, is

where $\Delta \nu$ is the line width, and D is the distance to the source.

Substituting Eq. (3.5.1) for I, Eq. (3.4.5) for J_s and Eq. (3.5.3) for τ_0 into Eq. (3.5.4), considering that $l d\sigma = dV_s$ is the elementary volume from which the saturated maser emission comes to the observer, and integrating over the whole volume providing this emission, we get:

$$F_s = \int dF_s = \frac{h\nu}{D^2} \frac{\delta}{\Omega} \int N_1' b_1 \beta_{12} dV_s . \qquad (3.5.5)$$

In obtaining this equation we have also used the common relation between the Einstein's A and B coefficients.

It is straightforward to obtain an analogous equation for the flux due to optically thin spontaneous emission:

$$F_{sp} = \int dF_{sp} = \frac{h\nu}{D^2} \frac{A_{21}}{4\pi} \int N_2' b_2 dV_{sp} . \qquad (3.5.6)$$

Deviding Eq. (3.5.5) over Eq. (3.5.6), we get:

$$\frac{F_s}{F_{sp}} = \frac{4\pi}{\Omega} \frac{\delta}{\Omega} \frac{\int N_1' b_1 \beta_{12} dV_s}{\int N_2' b_2 dV_{sp}} \,. \tag{3.5.7}$$

Of the three ratios composing the right-hand side of Eq. (3.5.7) two are obvious — the ratio of the integrated numbers of emitting particles and the ratio of the solid angles of emission (4π for spontaneous emission and Ω for maser emission). The third ratio, δ/A_{21} is the ratio of the rates of emission, per particle per second. The rate of the saturated maser emission is δ because it is determined by the collisional "recycling" of the primary radiative-radiative pumping (cf. Paper 2). If the observed maser amplification occurs at the optimum gas density, N_e^{max} , δ is obtained by combining Eqs. (3.4.4) and (3.1.4):

$$\delta \approx 2 \cdot 10^7 \, n^{-0.7} \,. \tag{3.5.8}$$

Using the approximation for A_{21} mentioned in Sect. 3.4, we find

$$\frac{\delta}{A_{21}} \approx 4 \cdot 10^{-3} \, n^{4.3} \, . \tag{3.5.9}$$

Eq. (3.5.9) shows that the factor δ/A_{21} strongly favors high n transitions. The physical reason for this can be roughly explained as follows. As is shown in Paper 2, N_e^{max} is close to the density of thermalization, the density under which the *net* rate of collisional transitions across the levels in question, $\approx \delta (kT_e/h\nu_0)$, surpasses the net rate of spontaneous radiative transitions which is roughly $\sim A_{21}$. Thus, close to the density of thermalization, $\delta/A_{21} \sim (kT_e/h\nu_0) \propto n^3$. This explains, very roughly, of course, why the δ/A_{21} factor in Eq. (3.5.7) favors high n levels.

The forgoing result is important for our prognosis of the observability of HRL lasers. If there is a gradient of density in the source, and hence the spontaneous emission in a line comes not only from the region favorable for lasing in this line, the ratio of the integrals in Eq. (3.5.7) can be $\ll 1$. It is seen then from Eqs. (3.5.7) and (3.5.9) that at small n saturated laser emission can not significantly exceed spontaneous emission in principle, unless the solid angle of lasing is $\Omega \ll 1$. This greatly narrows the conditions of laser detectibility: the source has either to be homogeneous in density (this density being just optimum for lasing in a chosen line), and/or the solid angle of the laser beam must be very small, requiring a special source geometry. Of course, to be detected in a small solid angle such a laser must also have a fortuitous orientation with respect to the observer. If these conditions are not fulfilled, the laser emission will either be lost in a bright spontaneous background or will miss the observer geometrically.

In the particular case of the model masing disk of MWC349, the solid angle of masing, given by Eq. (3.4.7), does decrease with decreasing n, but it decreases slower than δ/A_{21} does [Eq. (3.5.9)], thus, after masers have become fully saturated, i.e. for $n \lesssim 20$, the contrast F_s/F_{sp} should drop with decreasing n, and at some value of n the laser component should vanish in the brighter background of spontaneous emission. We can crudely estimate this value of n as follows. Taking as F_s/F_{sp} for 21α the ratio of the observed maser flux, shown in Fig. 1, to the level of the spontaneous flux given in this figure by the solid theoretical curve, $F_s/F_{sp} \approx 10$, we find, from $F_s/F_{sp} \propto n^{2.4}$ [Eqs. (3.5.7), (3.4.7), and (3.5.9)], that F_s/F_{sp} drops to ≈ 1 at $n \approx 8$. This agrees with the lack of a significant lasing component at $n \lesssim 10$ in Fig. 1.

3.6. Saturation and the (Peak Separation) - (Line Frequency) Relation

Proper accounting for saturation may help solve one more puzzle associated with the multi-line HRL maser in MWC349. It was observed that the peak separation δv increased with the decreasing n in double-peaked masing $n\alpha$ -lines — from $\approx 40~\rm km\,s^{-1}$ at 36α and 35α to $\approx 50~\rm km\,s^{-1}$ at 30α (Thum $et\,al.$ 1992; 1995). This seemed to be in accord with the idea that higher frequency lines should mase at higher density, thus closer to the center of the Keplerian disk where the rotation velocity is faster. However, attempts to explain the $\delta v(n)$ correlation quantitatively, assuming a regular density structure in the disk, met with difficulties. Ponomarev $et\,al.$ (1994) argued that the observed ratio $\delta v(30\alpha)/\delta v(35\alpha)$ would require an improbably steep radial gradient of density ($\alpha \gtrsim 4~\rm in~N_e \propto r^{-\alpha}$), if each line mased at its density of maximum unsaturated gain. The recently discovered 26α and 21α (Thum $et\,al.$ 1994a,b) are even closer in their peak separation to each other and to 30α (all have $\delta v \approx 50~\rm km\,s^{-1}$), so that very unacceptable density gradients ($\alpha \sim 10-70$) are required to realize them at their densities of maximum unsaturated gain in a Keplerian disk.

To explain the levelling off of $\delta v(n)$, Thum $et\,al.$ (1994b) proposed that the disk rotation curve itself levels off inside some radius. No physical mechanism for such levelling off in a circumstellar disk is, however, proposed. Also improbable is the hypothesis that the ionized disk "finishes" abruptly at $R\sim 40\,\mathrm{A.U.}$ from the star, where $N_e\sim 10^7-10^8\,\mathrm{cm^{-3}}$, so that all the submm lines are forced to form at this high-density edge. At least, it is certainly not the case in the Hollenbach $et\,al.$ (1994) photoevaporation disk model we adopt here.

We hypothesize instead that the clustering of submm lines in some ring of the disk to produce close values of δv , is due to their interaction via saturation. The forgoing analysis was based on the assumption that masers and lasers in different lines are formed independently from each other, at their densities of maximum unsaturated amplification. Yet, only for the lowest n lines are the regions of maximum unsaturated amplification well separated in the model disk of MWC349 — the higher the n, the more the amplification regions for adjacent lines should overlap (Fig. 2). We argued above that the disk masers and lasers with $n\lesssim 30$ are affected by saturation. A possible mechanism for a maser to change its location under the influence of another saturated maser was described in Paper 2. Saturation in a masing line increases the decay rate of its upper level, thereby facilitating energy sink for the adjacent line above. As a result, the latter is able to mase at a higher density than its density of maximum unsaturated masing, with the consequence that adjacent lines will cluster spatially. One can suppose that this effect in MWC349 is initiated by some lasing saturated IR transition below 21α , at a density $\sim 10^8 \, \mathrm{cm}^{-3}$, where the overlapping of negative absorption coefficients for this group of transitions becomes large enough. A verification of this mechanism by direct numerical simulation is under way.

4. THE PEDESTAL COMPONENT

4.1. Masing in the Outflow?

Some evidence for masing in the pedestal component of HRL, as opposed to the double-peaked component, has appeared lately.

Martín-Pintado et al. (1994a) observed narrow, highly variable, and therefore presumably masing features in 39α and 35α at "non-double-peak" radial velocities which they ascribe to the outflow. In addition, Martín-Pintado et al. (1994b) argued that the observed flux in 66α (which, like all the other

lines with $n \stackrel{>}{_{\sim}} 36$, has only a pedestal component) was considerably higher than the expected spontaneous emission, and hypothesized that it was due to maser amplification.

Thum et al. (1994b) find that the pedestal in 21α is relatively stronger than in 26α and attributed this to effects of stimulated emission in the outflow. Their observation of these two lines is plotted in Fig. 1, and it is seen indeed that there is a significant excess of the flux, relative to the probable optically thin LTE value, for both the double-peaked and the pedestal components, especially in the case of 21α .

Thum et al. (1995) find that the pedestal flux ratios of several β/α pairs of nearly the same frequency — from $26\alpha/33\beta$ to $40\alpha/48\beta$ — are considerably smaller than the expected optically thin LTE ratios, and explained the relative enhancement of the α -lines by the stimulated emission in the outflow.

In view of this observational evidence, it is interesting to investigate the conditions of masing in the outflow of MWC349, as compared with its disk. The radio continuum data for this source are adequately explained by a model of spherically-symmetric expansion at constant velocity (Olnon 1975). Adopting the value of the outflow constant obtained by Cohen *et al.* (1985), $N_e(R) R^2 = 0.81 \cdot 10^{37} \,\text{cm}^{-1}$ (which corresponds to the spherically symmetric, 50 km s⁻¹ constant velocity mass loss of $1.2 \cdot 10^{-5} \,\text{M}_{\odot}/\text{yr}$), we will have for the radius $R(N_e)$ at which the outflow has a given electron number density N_e :

$$R(N_e) \approx 2.8 \cdot 10^{18} N_e^{-0.5}$$
 (4.1.1)

The values of k_{net}^{max} presented in Table 1 of Paper 2, were calculated for the thermal line broadening alone, at the temperature considered. To account for the line weakening due to the expansion of the outflow, these values should be decreased by a factor of $\approx w/\Delta v_D$, where w is the observed line width, due to expansion, and Δv_D is the thermal Doppler line width. Thus, in this case maser gain is

$$|\tau^{max}| \approx |k_{net}^{max}| R(N_e^{max}) \left(\Delta v_D/w\right). \tag{4.1.2}$$

If masing for each line occurs in its "optimum" layer $(N_e = N_e^{max})$, Eqs. (4.1.1) and (4.1.2), and Table 1 of Paper 2, with $w/\Delta v_D \approx 4$, yield the following estimates for the maser gain at the lowest conceivable temperature, $T_e = 5,000$ K: $|\tau|(21\alpha) = 7$; $|\tau|(30\alpha) = 1.8$; $|\tau|(40\alpha) = 0.4$; $|\tau|(66\alpha) = 0.02$; $|\tau|(92\alpha) = 0.002$. These values decrease with increasing T_e : at $T_e = 10,000$ K, $|\tau|$ is > 1 for only $n \lesssim 21$.

These estimates show that maser gain > 1 in the outflow is only possible for relatively low $n \approx 0$ -lines, $n \lesssim 30 \, (\pm 10)$, with the exact values depending on the temperature.

At longer wavelengths ($n \gtrsim 30$), Fig. 1 shows a gradually increasing depression of the pedestal fluxes, as compared with the "simple" optically thin LTE model. This model (solid lines in Fig. 1) assumes that radiation in all recombination lines comes from the same volume of space. Then the flux is simply proportional to spontaneous emissivity, which is $\propto n^{-6}$ for $n \gg 1$. However, as can be seen in Fig. 10 of Paper 2, the free-free opacity surpasses the line opacity at $n \gtrsim 30$, and their ratio then steeply increases with n (k'_l in this figure should be reduced by the factor $w/\Delta v_D \approx 4-6$ to account for the velocity dispersion in the outflow). Therefore, for the long wavelength lines only emission from the volume located above the surface $\tau_c \approx 1$ will be observed. In the approximation of a spherically symmetric, constant velocity outflow with $N_0 R_0^2 = 0.81 \cdot 10^{37} \, \mathrm{cm}^{-1}$ and $T_e = 10^4 \, \mathrm{K}$, the radius at which $\tau_c = 1$ is

$$R(\tau_c = 1) \equiv R_0 \approx 2.4 \cdot 10^{16} \left(\frac{\nu}{\text{GHz}}\right)^{-2/3} (\text{cm}) ,$$
 (4.1.3)

and the volume emission measure above the level $\tau_c = 1$ is

$$\int N_e^2 dV = N_0 R_0^2 \cdot 4\pi \int_{R_0}^{\infty} \frac{dR}{R^2} \approx 8.0 \cdot 10^{74} R_0^{-1} \approx 3.4 \cdot 10^{58} \left(\frac{\nu}{\text{GHz}}\right)^{2/3} \propto n^{-2} . \tag{4.1.4}$$

Thus, the luminosity and the flux in the lines with $n \gtrsim 30$ should be proportional to $n^{-6}n^{-2} \propto n^{-8}$. This prediction is shown in Fig. 1 with a broken line. It describes quite well the observed fluxes from the outflow for the whole range $n \approx 30-92$. The greatest deviation from this theoretical curve (a factor of ≈ 4 excess) is the observation of 66α by Martín-Pintado et al. (1994b). These authors concluded that maser amplification in 66α (of about this factor) takes place in the outflow and they support this conclusion by model calculations, assuming a mass outflow rate of $9 \cdot 10^{-5} \,\mathrm{M}_{\odot} \,\mathrm{yr}^{-1} - 8$ times higher than the value of Cohen et al. (1985) adopted here. With the latter, as argued above, the negative optical depth of the outflow in 66α is only $\sim -10^{-2}$, and masing with a gain > 1 is impossible. The 66α flux measured by

Altenhoff *et al.* is significantly lower and closer to our theoretical curve. More observations in this line are needed to clarify the possibility of time variations and masing.

4.2. Masing Disk versus Masing Outflow

We showed in the preceding section that only HRL with $n \lesssim 30 \pm 10$ can have maser gain $\gtrsim 1$ in the model spherically-symmetric outflow with the mass loss rate of MWC349. However, lines with $n \lesssim 40$ require $N_e \gtrsim 5 \cdot 10^6$ cm⁻³ for their masing (see Table 1 in Paper 2). According to Eq. (4.1.1), these high densities would occur in the outflow only at $R \lesssim 1 \cdot 10^{15}$ cm. Yet, in the photoevaporation disk model adopted here, there is no outflow so close to the star: the quasi-static disk's atmosphere extends up to $R = R_q \approx 3 \cdot 10^{15}$ cm for a star of 26 M_{\odot} (Sect. 3.1).

We conjecture therefore that the pedestal masing, especially masing with a gain > 1, as in the 26α and 21α lines, occurs in the disk of MWC349, rather than in its outflow.

The optical thickness of the disk increases with decreasing n. It was demonstrated in Sect. 3.2 that a dominant double-peaked component first appears at $\approx 36\alpha$ where gain in the chords can be ≈ 1 . But when this happens, the lower n lines in the outer parts of the disk already have their gains approaching unity and can therefore undergo a weak amplification. For example, at the physical edge of the static atmosphere $(R=R_g)$, where $N_e\approx 4\cdot 10^6\,\mathrm{cm}^{-3}$, the 40α line would have $\tau\sim 1$, if its amplification path length is $\sim R_g$; its weak amplification could thus produce some structureless supplement to the spontaneous emission. Amplified emission from the different radial velocities within the disk (see Fig. 1 in Paper 1) which form the "pedestal" component should progressively increase with increasing $|\tau|$ and decreasing n. This is in accord with the decrease of the $(\beta/\alpha)^{spont}/(\beta/\alpha)^{obs}$ ratio toward lower n, seen in the Thum $et\,al$. (1995) paper and suggestive of an increase in the α -line pedestal amplification with decreasing n.

At still lower n, not only the chords (which give the double-peaked component) but also other parts of the disk acquire maser gain sufficient for high gain masing, and they will form an ever growing masing "pedestal" to the double-peaked component. This disk-originated pedestal can be broad, because of the radial velocity dispersion in the disk. The contrast between the double-peaked component and the pedestal should decrease with increasing saturation. Our numerical modeling of the masing in an edge-on Keplerian ring (Paper 1) shows that in a fully saturated regime the center-to-peak intensity ratio may increase up to $I_c/I_{pk} \approx 0.5$. The increase of I_c/I_{pk} from ≈ 0.06 by 26α up to ≈ 0.2 by 21α , as observed by Thum et al. (1994b), is in good agreement with this model, given the evidence of a growing degree of saturation with decreasing n. We anticipate a further decrease of the peak-to-center intensity ratio with decreasing n, due to the increasing saturation in the disk, before spontaneous emission washes out both the double-peaked and the "pedestal" masing components, at $n \approx 10$.

5. β -LINES

Five recombination β -lines of hydrogen have been detected in MWC349 so far: 39 β (Gordon 1994), 48 β , 38 β , 33 β , and 32 β (Thum *et al.* 1995). Comparison of the intensities of α/β pairs proved to be an effective tool in analyzing masing in α -lines. Besides, β -lines themselves show some evidence of increasing masing with increasing frequency, and it appears likely a real high-gain maser in the higher frequency β -lines will be detected in the near future. These two aspects of studying β -lines in MWC349 are discussed below.

5.1. β/α Intensity Ratio

Gordon (1994) detected the first β -line in MWC349 (39 β), and he was the first to use a β/α intensity ratio (39 $\beta/31\alpha$, the lines of approximately equal frequencies), as evidence of masing — in the 31 α double-peaked component.

Thum et al. (1994c) used the β/α intensity ratios of several other equal-frequency pairs they had detected, and demonstrated weak masing in the α -line pedestals (see Sect. 4).

The use of the β/α ratio is based on the assumption that both lines of the pair are produced in approximately the same region of space, and on the fact that $|k_{net}^{\alpha}|$ is normally several times higher than $|k_{net}^{\beta}|$. Because of the latter condition, the medium always becomes optically thick in the α -line first. Note that the relative effects of optical thickness are just opposite when the populations are inverted and when they are not. In the former case the β/α intensity ratio changes in favor of the α -line, because of the higher maser amplification. In the latter case the ratio changes in favor of the β -line, as compared with the optically thin case, because of the higher self-absorption in the α -line. Since in the β/α method the observed intensity ratio is compared with the spontaneous emissivity ratio, it is useful to have a simple approximation for the latter. We derive such an approximation in Appendix 2.

For the two pedestal pairs, $39\beta/40\alpha$ and $39\beta/31\alpha$, Gordon (1994) measured intensity ratios of ≈ 0.6 and 0.12, respectively. Using, as the corresponding spontaneous emissivity ratios, $\epsilon(39\beta)/\epsilon(40\alpha) \approx 0.6$ and $\epsilon(39\beta)/\epsilon(31\alpha) \approx 0.3$, he came to the conclusion that these lines were observed in an approximately LTE optically thin ratio. Our Eq. (A2.5) gives for the $\epsilon(39\beta)/\epsilon(40\alpha) \approx 1.3$ — twice as much as the value adopted by Gordon. Comparison of our emissivity ratios with the flux ratios observed by Gordon leads us to the conclusion that both α -line pedestals are amplified by a small factor of ≈ 2 . We note a remarkably good agreement of our $(\beta/\alpha)^{spont}/(\beta/\alpha)^{obs}$ ratio for the $39\beta/40\alpha$ pair with the Thum's et al. (1995) ratio for the $48\beta/40\alpha$ pair: ≈ 0.5 in both cases. This is another confirmation that the 40α pedestal is amplified by a factor of ≈ 2 (see Sect. 4.2).

5.2. β -Line Masing in the Disk

The highest frequency β -line detected so far in MWC349, 32 β , is also the only one demonstrating a double-peaked component along with the broad pedestal component (Thum et al. 1995). By analogy with the double-peaked α -lines, the double-peaked component of 32 β was interpreted by Thum et al. (1995) as a result of weak masing in the disk. Here we develop this interpretation further.

First of all, using the rather precise information about the peaks' radial velocities (Table 2 in Thum $et\,al.$), we argue that the 32β peakes were formed in the same region where the α -line with the closest observed n (34α) was formed, rather than in the region where the 32β frequency companion (26α) was formed. The red peak of 32β ($33.6 \pm 2.3\,\mathrm{km\,s^{-1}}$) is closer to that of 34α ($32.3 \pm 1.0\,\mathrm{km\,s^{-1}}$, as averaged for a long period of observations; Thum $et\,al.$ 1994a) than to that of 26α ($30.7 \pm .1\,\mathrm{km\,s^{-1}}$), though the difference (2-3 km s⁻¹) is comparable with the observational errors or time variations (1-2 km s⁻¹). Yet, the blue peak of 32β ($-13.3 \pm 1.5\,\mathrm{km\,s^{-1}}$) is much closer to that of 34α ($-13.0 \pm 1.5\,\mathrm{km\,s^{-1}}$) than to that of 26α ($-21.1 \pm .1\,\mathrm{km\,s^{-1}}$), and in this case the difference between the two groups ($\approx 6\,\mathrm{km\,s^{-1}}$) is significantly greater than the uncertainties ($\pm 2\,\mathrm{km\,s^{-1}}$).

If the two lines are indeedcoming from the same volume of space, masing seems to be necessary to explain their observed flux ratio. From Eq. (A2.5) we have:

$$\frac{\epsilon_{32\beta}}{\epsilon_{34\alpha}} \approx 1.6 \ . \tag{5.2.1}$$

Yet, the fluxes in the peaks of 32β ($2 \pm 2 \,\mathrm{Jy\,km\,s^{-1}}$) and 34α ($20 \pm 20 \,\mathrm{Jy\,km\,s^{-1}}$) have a ratio of only ~ 0.1 , though with a high uncertainty. The theoretical optically thin ratio (5.2.1) is thus much higher than the observed ratio; this discrepancy is naturally explained by maser amplification which is stronger in 34α than in 32β .

That masing α - and β -lines with close n can indeed share the same region of space, can be shown in the following general manner. Every three adjacent levels, 1, 2, and 3 (Fig. 3) produce two α -lines (2-1 and 3-2) and one β -line (3-2). The definition of excitation temperature [Eq. (2.2.1) in Paper 2] and the obvious identity (N_1g_2/N_2g_1) (N_2g_3/N_3g_2) $(N_3g_1/N_1g_3) = (n_1/n_2)$ (n_2/n_3) $(n_3/n_1) = 1$ give the following relation between the frequencies and excitation temperatures of the three transitions (Strelnitski 1983):

$$\frac{\nu_{31}}{T_{x31}} = \frac{\nu_{21}}{T_{x21}} + \frac{\nu_{32}}{T_{x32}} \ . \tag{5.2.2}$$

Since β -coefficients of the adjacent α -lines, and, therefore, the excitation temperatures T_{x21} and T_{x32} , are always close to each other [see eqs. (2.2.3) and (2.2.4) and Fig. 4 in Paper 2], and since $\nu_{31} = \nu_{21} + \nu_{32}$,

it follows from Eq. (5.2.2) that

$$T_{x31} = T_{x21} \frac{\nu_{31}}{\nu_{21} + \nu_{32} \frac{T_{x21}}{T_{x22}}}$$

should also be close to T_{x21} and T_{x32} . Thus, the $\beta(N_e)$ and the $k_l(N_e)$ profiles should be similar for the α - and β -lines of close n. The $k_{net}(N_e)$ profiles will also be similar for those lines with $k_l \gg k_c$ ($n \lesssim 40$; see Fig. 8 in Paper 2).

Fig. 6 in Paper 2 shows indeed that the k_{net} (N_e) profiles are quite similar for the α - and β -lines of close n. The $k_{net}^{32\beta}/k_{net}^{34\alpha}$ ratio, at the density of their maximum gain ($N_e \approx 1.5 \cdot 10^7 \, \mathrm{cm}^{-3}$) is ≈ 0.2 , at $T_e = 5{,}000 - 10{,}000 \, \mathrm{K}$. Suppose, $\tau_{net}^{34\alpha} \approx -3$. Then $\tau_{net}^{32\beta} \approx -0.6$, and their intensity ratio, produced by unsaturated amplification, will be $\approx \mathrm{e}^{\Delta\tau} \approx 10$, as observed. According to Fig. 5, Paper 2, to produce these optical depths at $10{,}000 > T_e > 5{,}000 \, \mathrm{K}$ an amplification length of $50 - 100 \, \mathrm{A.U.}$ would be sufficient, again in accordance with the interferometric distance of 80 A.U. between the 30α hot spots (Planesas $et \, al. \, 1992$).

If the model of a masing Keplerian disk, with density increasing toward the center, is correct, then 32β should be the "threshold" of masing for β -lines, as 36α is for α -lines (Thum *et al.* 1995). The value of the maximum $|k_{net}|$ is about an order of magnitude smaller for a β -line than for an α -line of close n, which is why at the radial distance where the "threshold" α -line is formed the corresponding β -lines are still optically thin and thus not amplified enough. The threshold β -line, with $|\tau_{net}| \approx 1$, should appear at a smaller radial distance (higher density), where the corresponding α -line is already optically thick. This explains why the threshold of double-peaked masing occurs at smaller n for β -lines (32 β) than for α -lines (36 α).

The intensity of double-peaked masing in β -lines should increase further with decreasing n, as happens among α -lines. Using Fig. 6g of Paper 2 and Eq. (3.1.5) of this paper, we find, for example, that the maser gains of the 29β and 26β lines (both having good conditions for ground-based observations) should be, respectively, ≈ 1.5 and 2.5 times higher than the gain in 32β . Hence, maser amplification several times stronger in 29β and 26β lines is anticipated. Detection of a masing double-peaked component in these lines, which have very close observed α -companions (29α — 30α and 26α — 27α , respectively), will be especially useful for a comparative analysis similar to that presented for the $32\beta/34\alpha$ pair in Thum et al. (1995) and in this section.

Suborbital and orbital IR observatories have a good chance of detecting, in the near future, even stronger lasers in higher frequency β -lines — from $\approx 20\beta$ through $\approx 15\beta$ ($\approx 200-100\mu$ m), where the unsaturated maser gains can be considerably higher than unity.

In conclusion, we emphasize once more that an important difference exists between the traditional analysis of optically thin α/β pairs and the new situation where masing is responsible for the observed intensities: a "close frequency" pair is preferable in the first case, while a "close n" pair — in the second.

6. CONCLUSION

MWC349 is the only source in which strong HRL masers have been detected; moreover, it is a stellar source in which most HRL α -transitions (both masing and non-masing) have been observed — more than twenty! This provides us a unique opportunity to study in detail the conditions needed for high gain HRL masing in the larger general context of HRL emission. Such a study was undertaken in this paper and Paper 2, and can be summarized as follows:

- (1) The factor N_e^2 plays a decisive role in determining the gain $|\tau|$ of an HRL maser.
- (2) At high principal quantum numbers n, the practical creation of a high gain HRL maser is hindered by the large dimensions needed to make $|\tau| > 1$, a requirement caused by the low densities involved in inverting high n transitions, and by free-free absorption which reduces the gain.
- (3) Low n transitions require high densities for inversion, and if present in a source (as is the case for MWC349), the unsaturated gain may become very large even with small dimensions. However, masers or lasers at low n saturate easily, and tend to disappear in the background of the spontaneous emission of the source unless the solid angle of the maser beam is very small.
- (4) In the case of MWC349 the optimum interval for strong α -line masing and lasing lies between these two extremes, $10 \lesssim n \lesssim 36$. Relatively strong, double-peaked IR α -line lasers may, therefore, be discovered in this source in the interval $n \approx 10-20$. Their expected fluxes can be estimated from Fig. 1.

- (5) A $|\tau| > 1$ α -line maser in the *outflow* of MWC349 doesn't seem possible for $n \stackrel{>}{\sim} 30$ –40.
- (6) Fig. 1 confirms the hypothesis of Thum $et\,al.$ (1994b) that the relative increase of the pedestal component in 26α and 21α is due to masing. But we show the observed pedestal masing probably occurs in the disk, not in the outflow. We predict further increase of the pedestal-to-peak flux ratio toward lower n, until at $n\approx 10$ the whole structure is lost in the steeply growing spontaneous emission of the source.
- (7) High-gain, double-peaked β -line masers and lasers with n < 32 should be present in the submm and IR domain, with 29β (614 μ m) and 26β (447.4 μ m) being the best candidates for the ground-based searches.
- (8) β/α line pairs of close n transitions are more informative in the case of masing than the close-frequency line pairs.

APPENDIX 1: Prof of the Need for Masing

Though the hypothesis of maser amplification in the mm and submm HRL in MWC349 is now widely accepted, paradoxically enough no strict proof for this has yet been given. In this Appendix we briefly review the existing attempts to prove maser action occurs in these lines. We demonstrate their insufficiency, and propose a more rigorous proof.

The high intensities of the double-peaked lines — higher than one would expect if the emission were purely spontaneous — was the primary reason to suspect maser amplification (Martin–Pintado $et\,al.$ 1989a). These authors demonstrated, by model calculations, that the observed intensity of 30α , for example, could not be produced by thermalized emission from the expanding envelope of MWC349, the location where the lower frequency recombination radio lines were thought to arise. However, it is known now that the double-peaked lines do not originate in this outflow, so this modeling can no longer be taken as a proof of their masing.

Martín–Pintado et al. (1989b) made an attempt to guess the size of the emitting "hot spots", with the (rather arbitrary) assumption that the upper limit of the size is defined by the observed time scale of the intensity variations and the maximum observed velocity of the gas motions around the star. They obtained a size of $\lesssim 4 \cdot 10^{14} \, \mathrm{cm}$ which, at the distance of 1.2 kpc (Cohen et al. 1985), corresponds to an angular size of $\lesssim 0.022 \, \mathrm{arcsec}$. The observed flux densities then give a brightness temperature in the hot spot of $T_b \gtrsim 1 \cdot 10^6 \, \mathrm{K}$ — implying some amplification, because the highest conceivable brightness temperature of the input radiation for the maser is less then $10^4 - 10^5 \, \mathrm{K}$.

Two more arguments were put forward in support of masing in these double-peaked lines: their time variability (Martı́n-Pintado et al. 1989b; Thum et al. 1992), and the narrowness of their spectral profile (Thum et al. 1992; Ponomarev et al. 1992). Both phenomena are more easily explained with the hypothesis of unsaturated maser amplification.

The last two arguments are, however, indirect, while the first two are based, respectively, on the incorrect association of these lines with the outflowing gas, and on a mere guess of the radiating region's size. Thus none of them can be taken as a strict proof of masing. Yet, the direct measurement of the angular separation between the two hot spots responsible for two spectral peaks in 30α (Planesas, Martín–Pintado, and Serabyn 1992) actually enable us to prove masing quite rigorously, as follows.

According to Planesas $et\,al.$ (1992) the angular distance between the centers of the two hot spots is $\theta_s=(0.065\pm0.005)$ arcsec = $(3.2\pm0.2)\,10^{-7}$ rad. This separation can serve as a strict upper limit to an individual hot spot's angular diameter, θ_d . If the separation between the two spectral peaks is due to the motions of the gas (which seems very probable), there should be some connection between the radial velocity scales and the geometrical scales. In particular, the narrowness of the peak's spectral width, Δv , as compared with the separation between the peaks, δv , ($\Delta v: \delta v \approx 1:4$), is an indication that the ratio of the linear diameter of a hot spot to the distance between the hot spots, $d: s = \theta_d: \theta_s$, should also be about 1:4. Our numerical modeling of maser amplification in an edge-on Keplerian disk (Ponomarev $et\,al.$ 1994) indeed gives $d: s \lesssim 0.3$. Thus, we can safely admit that at least $d^2 \ll s^2$ (or $\theta_d^2 \ll \theta_s^2$) is true.

Suppose that the observed flux F within one peak of the 30α double-peaked profile were due to isotropic, optically thin spontaneous emission. In this case

$$F = \frac{L_{sp}}{4\pi D^2} \,,\tag{A1.1}$$

where D is the distance to the source;

$$L_{sp} = N_2 A_{21} h \nu_0 V \tag{A1.2}$$

is the total spontaneous luminosity of the medium volume V with the upper state population N_2 ; A_{21} is the Einstein coefficient for spontaneous emission, ν_0 is the frequency of the transition, and h is the Planck constant. Unless the geometry of a hot spot is very unusual, its "vertical" dimension should also be $\approx d$ (or $\lesssim d$, as it can be in the case of an edge-on disk). Then

$$V \le d^2 l \ll s^2 l$$
, or $V \ll (\theta_s D)^2 l$, (A1.3)

where l is the extension of the emitting region along the line of sight. Combining equations (A1.1) – (A1.3) leads to the following strict limit for the integrated flux due to spontaneous emission:

$$F \ll \frac{A_{ji}}{4\pi} \theta_s^2 N_j l h \nu_0 . \tag{A1.4}$$

The population density of a hydrogen atom level with principal quantum number n is given by the Saha-Boltzmann equation:

$$N_n = \left(\frac{h^2}{2\pi m k T_e}\right)^{3/2} N_e^2 n^2 e^{\frac{I_n}{k T_e}} b_n , \qquad (A1.5)$$

where N_e is the electron number density; I_n is the ionization energy of the state n; b_n is the departure coefficient; k is the Boltzmann constant, and m is the electron mass. For $n \approx 30$, b_n is close to one if $N_e \gtrsim 10^6 \, \mathrm{cm}^{-3}$, and for the temperatures considered here, $3000\mathrm{K} \leq T_e \leq 10000\,\mathrm{K}$ the factor $\mathrm{e}^{\frac{I_n}{kT_e}}$ is very close to one too. Thus, we have for the n=30 level:

$$N_n \approx 4 \cdot 10^{-19} N_e^2$$
 (A1.6)

Substituting into Eq. (A1.4): $A_{31,30} \approx 225 \,\mathrm{s}^{-1}$, together with the Eq. (A1.6) and with the observed value $F_{30\alpha} \approx 1 \cdot 10^{-14} \,\mathrm{\frac{erg}{cm^2 s}}$ (Thum *et al.* 1992), we obtain finally the following strong requirement for the emission measure:

$$N_e^2 l \gg 1 \cdot 10^{31} \text{ cm}^{-5}$$
 (A1.7)

For a Keplerian disk $l \lesssim s$ (Ponomarev *et al.* 1994). With the above interferometric value of θ_s and with the distance to the source $D=1.2\,\mathrm{kpc}$, we have $l \lesssim s=\theta_s D=1.2\cdot 10^{15}\,\mathrm{cm}$. Then another strong requirement, for the electron density, follows from Eq. (A1.7):

$$N_e \gg 9 \cdot 10^7 \,\mathrm{cm}^{-3}$$
 (A1.8)

We emphasize that (A1.7) and (A1.8) are *strong* inequalities, becose of the probable small size of d, as compared with s. But even these lower limits for $N_e^2 l$ and N_e are high enough to show the model of optically thin spontaneous emission is internally contradictory.

Indeed, if the 30α line were due to optically thin spontaneous emission alone, the observed line width, $\Delta v \approx 12 \,\mathrm{km \, s},^{-1}$ corresponds to a kinetic temperature $T_e \approx 3000 \,\mathrm{K}$. The Rayleigh-Jeans approximation is valid for mm lines, and the optical depth in a line of spectral width $\Delta \nu$ is given by (Lang 1974):

$$\tau_{ij} \approx \frac{\pi e^2}{mc} f_{ij} \frac{N_i}{\Delta \nu} \frac{h\nu}{kT_x} b_n l , \qquad (A1.9)$$

where T_x is the excitation temperature of the transition. At the densities set by Eq.(A1.8) the 30α transition should be deeply thermalized (see Fig. 6b in Paper 2). With $\Delta\nu\approx\nu_0\cdot\frac{\Delta v}{c}\approx9\cdot10^6$ Hz (and, correspondingly, $T_x=T_e\approx3000$ K), and with the oscillator strength for hydrogen α -transitions being $f_n^{\alpha}\approx0.194n$ (Menzel 1969), we have

$$\tau_{ij} \approx 8 \cdot 10^{-31} N_e^2 l$$
 (A1.10)

Substituting (A1.7) for $N_e^2 l$ gives $\tau \gg 1$ which contradicts our assumption of optical thinness; thus this explanation of the observed value of $F(30\alpha)$ is contradicted.

Let us suppose instead that the 30α line is thermalized and optically thick. In this case the flux density in the line center is

$$S_{max} \approx B(\nu_0, T_x) \cdot \theta_d^2 \ll B(\nu_0, T_x) \cdot \theta_s^2 , \qquad (A1.11)$$

where $B(\nu_0,T_x)$ is the Planck function. Substituting into Eq. (A1.11): $B(232\,\mathrm{GHz},3000\,\mathrm{K})\approx 5\cdot 10^{-11}\,\mathrm{erg/(cm^2\,s\,Hz\,sr)},$ and $\theta_s^2\approx 1.0\cdot 10^{-13}\,\mathrm{sr},$ we obtain, as an upper limit for the possible flux density: $S_{max}\ll 0.5\,\mathrm{Jy},$ much less than the observed value, $S\approx 25\,\mathrm{Jy}.$

We conclude that neither optically thin nor optically thick spontaneous emission alone can explain the observed flux density and integrated flux in 30α , and, therefore, maser amplification of the line in an optically thick inverted medium is necessary.

APPENDIX 2: Spontaneous Emissivity Ratios for β/α Line Pairs

The integrated spontaneous emissivity in the line, whose lower and upper states' principal quantum numbers are, respectively, l and u, is

$$\epsilon_{ul} = \frac{h\nu_0}{4\pi} N_u A_{ul} , \qquad (A2.1)$$

where h is the Planck constant, ν_0 is the transition frequency, N_u is the upper state level population,

$$A_{ul} = 7.5 \cdot 10^{-22} \nu_0^2 f_{lu} \left(\frac{l}{u}\right)^2 \tag{A2.2}$$

is the Einstein coefficient, and f_{lu} is the oscillator strength.

The transition frequency is given approximately by $2cR/l_{\alpha}^{3}$ for α -transitions and $4cR/l_{\beta}^{3}$ for β -transitions, with R being the Rydberg constant (Lang 1974). Thus

$$\frac{\nu_{0\beta}}{\nu_{0\alpha}} \approx 2 \left(\frac{l_{\alpha}}{l_{\beta}}\right)^3. \tag{A2.3}$$

We emphasize that the values of l and u for the α transition may differ from those of the β -transition in an α/β pair.

When the upper levels of the α - and β -transitions are different, but not too distant, we obtain from Eq. (A1.5), ignoring the small difference in the factor $e^{\frac{I_n}{kT_e}}$:

$$\frac{N_{u_{\beta}}}{N_{u_{\alpha}}} \approx \left(\frac{u_{\beta}}{u_{\alpha}}\right)^2 \frac{b_{n(u\beta)}}{b_{n(u\alpha)}}.$$
(A2.4)

With $f_{lu} \approx 0.194l$ for α -lines, $f_{lu} \approx 0.027l$ for β -lines (Menzel, 1969), we have finally from Eqs. (A2.1) through (A2.4):

$$\frac{\epsilon_{\beta}}{\epsilon_{\alpha}} \approx 1.1 \left(\frac{l_{\alpha}}{l_{\beta}}\right)^{6} \frac{b_{n(u\beta)}}{b_{n(u\alpha)}}.$$
(A2.5)

If both l_{α} and l_{β} are $\gg 1$ and $|l_{\alpha} - l_{\beta}| \lesssim 10$, the uncertainty of this approximation is $\lesssim 10\%$, even if the b_n ratio is set equal to unity.

For the particular case of a pair of α - and β -lines of close frequencies, the condition $\nu_{0\alpha} \approx \nu_{0\beta}$, combined with Eq. (A2.3), implies $l_{\beta}/l_{\alpha} \approx 2^{1/3}$, and we get from Eq. (A2.5):

$$\frac{\epsilon_{\beta}}{\epsilon_{\alpha}} \approx 0.3 \qquad (\nu_{0\beta} \approx \nu_{0\alpha}) \ . \tag{A2.6}$$

V.P. thanks the partial support of this research by the Tomalla Foundation Fellowship and the International Center for Fundamental Physics in Moscow for its help in obtaining this Fellowship. VSS and VOP thank the Smithsonian Institution, National Air and Space Museum for a senior fellowship and visiting fellowship, respectively, to work in the Laboratory for Astrophysics on this program and related observations. Together with HAS they acknowledge financial support from the Institution's Scholarly Studies Program. HAS also acknowledges partial support from NASA grant NAGW-1711.

REFERENCES

Baker, J.G., and Menzel, D.H. 1938, Ap. J., 88, 52.

Brugel, E.W., and Wallerstein, G. 1979, Ap. J. (Letters), 229, L23.

Cohen, M., Bieging, J.H., Dreher, J.W., and Welch, W.J. 1985, Ap. J., 292, 249.

Goldberg, L. 1966, Ap. J., 144, 1225.

Gordon, M.A. 1992, Ap. J., 387, 701.

Gordon, M.A. 1994, Ap. J., 421, 314.

Greenstein, J. 1973, Ap. J., 184, L23.

Hamann, F., and Simon, M. 1986, Ap. J., 311, 909.

Hartmann, L., Jaffe, D., and Huchra, J.P. 1980, Ap. J., 239, 905.

Hollenbach, D., Johnstone, D., Lizano, S., and Shu, F. 1994, Ap. J., 428, 654.

Lang, K.R. 1974, Astrophysical Formulae, Springer Verlag.

Litvak, M.M. 1968, in "Interstellar Ionized Hydrogen," ed.: N.Y. Terzian, N.Y. – Amsterdam, Benjamin, p.713.

Martín-Pintado, J., Bachiller, R., Thum, C., and Walmsley, C.M. 1989a, Astr. Ap., 215, L13.

Martín-Pintado, J., Thum, C., Bachiller, R. 1989b, Astr. Ap., 229, L9.

Martin-Pintado, J., Neri, R., Thum, C., Planesas, P., and Bachiller, R. 1994a, Astr. Ap., 286, 890.

Martín-Pintado, J., Gaume, R., Bachiller, R., Johnston, K., and Planesas, P. 1994b, Ap. J. (Letters), 418, L79.

Olnon, F.M. 1975, Astr. Ap., 39, 217.

Planesas, P., Martín-Pintado, J., and Serabyn, E. 1992, Ap. J. (Letters), 386, L23.

Ponomarev, V.O., Smirnov, G.T., Strelnitski, V.S., Chugai, N.N. 1989, Astron. Tsirk., 1540, 5.

Ponomarev, V.O., Strelnitski, V.S., Chugai, N.N. 1991, Astron. Tsirk., 1545, 37.

Ponomarev, V.O., Smith, H.A., and Strelnitski, V.S. 1994, Ap. J., 424, 976 (Paper 1).

Smith, H.A., Strelnitski, V.S., Kelley, D., Lacy, J., and Miles, J. 1995, in preparation.

Strelnitski, V.S. 1974, Soviet Physics Uspekhi, 17, 507.

Strelnitski, V.S. 1983, Nauchnye Informatsii Astron. Council USSR ac. Sci., **52**, 75. (Spanish translation: Ciencia, **43**, 185.)

Strelnitski, V.S., Smith, H.A., Haas, M.R., Colgan, S.W.J., Erickson, E.F., Geis, N., Hollenbach, D.J., and Townes, C.H. 1995a, In: Proceedings of the Airborne Astronomy Symposium on the Galactic Ecosystem: From Gas to Stars to Dust, ed. M.R. Haas, J.A. Davidson, and E.F. Erickson; San-Francisco: ASP, 1995, p.271.

Strelnitski, V.S., Ponomarev, V.O., and Smith, H.A. 1995b, Ap. J., submitted (Paper 2).

Thompson, R.I., Strittmatter, P.A., Erickson, E.F., Witteborn, F.L., and Strecker, D.W. 1977, Ap. J., 218, 170.

Thum, C., Martín-Pintado, J., and Bachiller, R. 1992, Astr. Ap., 256, 507.

Thum, C., Matthews, H.E., Martín-Pintado, J., Serabyn, E., Planesas, P., and Bachiller, R. 1994a, Astr. Ap., 283, 582.

Thum, C., Matthews, H.E., Harris, A.I., Tacconi, L.J., Shuster, K.F., and Martin-Pintado, J. 1994b, Astr. Ap., 288, L25.

Thum, C., Strelnitski, V.S., Martín–Pintado, J., Matthews, H.E., and Smith, H.A. 1995, Astr. Ap., , submitted.

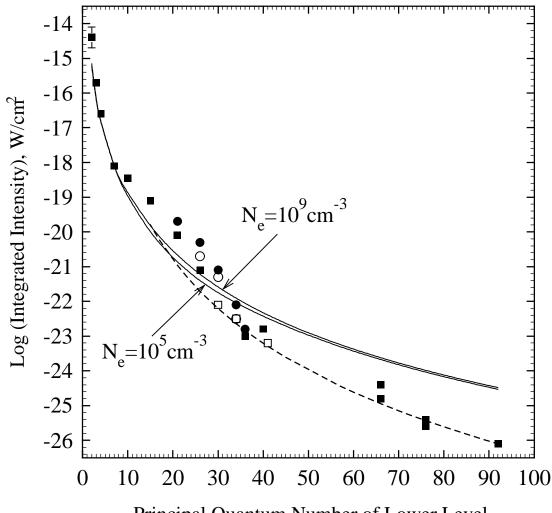
FIGURE CAPTIONS

- Fig. 1. Observed fluxes in hydrogen recombination α -lines in MWC349. *Dots*: the double-peaked component. *Squares*: the pedestal component, or an unresolved line. Filled symbols single measurements, either the only one—two known, the most reliable, or the brightest in a series. Open symbols averages for some period of time (Thum *et al.* 1992; 1994a). The observed values of flux for 2α , 3α , and 4α were corrected for extinction, in accordance with the Fig. 5 of Thompson *et al.* (1977). Error bars reflecting internal convergency are not shown: they are comparable to the symbol sizes for all observations. "Error bars" by $H\alpha$ show the amplitude of variations observed by Greenstein (1973) during one day (they were not intrinsic variations in MWC349-A see footnote ¹ in Brugel and Wallerstein, 1979). Two solid lines give, at two extreme values of N_e , the flux *ratios* predicted by the optically thin LTE model ("Case B", $T_e = 10,000$ K). The dashed line takes into account free-free absorption at low frequencies. Vertical position of all theoretical lines is arbitrary.
- Fig. 2. Location, within the model disk, of the annuli of maximum unsaturated amplification for $n\alpha$ lines. The values of n are indicated along the top "border" of the disk. The two "borders" give, in fact, only an idea of the disk's flare, showing the Log of the scale hight (in $1.8 \cdot 10^{10}$ cm) as a function of radius (in $1 \cdot 10^{12}$ cm). One quarter of the disk is only shown. The width of every annulus (at half maximum of k_{net}^{max}) is $\approx \pm 0.2$ in logarithm. Hence, in this logarithmic scale all the annuli have approximately the same width, and it is seen that overlapping of annuli should increase with increasing n.
- Fig. 3. To the explanation of the closeness of excitation temperatures (inversions) in α and β -lines of close n.

VLADIMIR S. STRELNITSKI: Laboratory for Astrophysics, MRC 321, National Air and Space Museum, Smithsonian Institution, Washington, DC 20560. *e-mail:* vladimir@wright.nasm.edu

HOWARD A. SMITH: Laboratory for Astrophysics, MRC 321, National Air and Space Museum, Smithsonian Institution, Washington, DC 20560. *e-mail:* howard@wright.nasm.edu

VICTOR O. PONOMAREV: Astro-Space Center of P.N. Lebedev Physical Institute, Leninsky prospect, 53, Moscow 117924. *e-mail:* ponomarev@rasfian.serpukhov.su



Principal Quantum Number of Lower Level

